Phase Diagrams of Poly(ethylene-*co*-vinyl alcohol) and Dimethylformamide Solutions Exhibiting Both Liquid–Liquid and Solid–Liquid Phase Separation

Juliana Aristéia De Lima, Maria Isabel Felisberti

Instituto de Química, Universidade Estadual de Campinas, 13083-970 - Campinas, São Paulo, Brasil

Received 28 January 2010; accepted 17 March 2010
DOI 10.1002/app.32483
Published online 7 June 2010 in Wiley InterScience (www.interscience.wiley.com).

ABSTRACT: The binary solutions of poly(ethylene-*co*-vinyl alcohol) (EVOH), with 38 and 32 wt % ethylene content, and *N*,*N*-dimethylformamide were submitted to experiments to determine the cloud temperature by optical microscopy and the dynamic crystallization temperature by differential scanning calorimetry (DSC). The thermally induced phase separation (TIPS) process was used with the EVOH/DMF solutions that showed liquid–liquid phase separation at temperatures higher than EVOH crystallization and with a decrease of the temperature-UCST behavior. The binary interaction model was applied to estimate the interaction energy densities (*B*) considering both intermolecular (ethylene-Et/DMF and vinyl alcohol-VA/DMF) and intramolecular (Et/VA) interactions. According to this model the liquid–liquid line for the EVOH-38/DMF solutions should be situated at higher temperatures in comparison with EVOH-32/DMF solutions. Moreover, the phase separation results from low affinity between the hydrophobic segments of EVOH and the segments of the copolymer containing hydroxyl or the solvent. The equilibrium melting temperature of EVOH increases with the increase of EVOH volume fraction in the solution. This effect is more pronounced for EVOH-32/DMF solutions, which means that there is an influence of the VA content in EVOH during the melting. © 2010 Wiley Periodicals, Inc. J Appl Polym Sci 118: 1787–1795, 2010

Key words: Poly(ethylene-*co*-vinyl alcohol); TIPS; iquid-liquid phase separation; crystallization

INTRODUCTION

Poly(ethylene-*co*-vinyl alcohol) (EVOH) copolymers show good thermal stability, high chemical resistance and have been used as a food packaging material because of their excellent gas barrier properties and harmlessness toward health. EVOH membranes have attracted interest from the fields of biomedical science and water treatment because of good blood compatibility and hydrophilicity,[1,2] respectively. These copolymers are essentially randomic and are semicrystalline over the entire range of composition, despite the irregularity and nonstereospecificity of the vinyl alcohol segments distributed in the EVOH copolymer chain.[3] Nevertheless, knowledge of EVOH phase behavior during technical processing is of considerable importance and, for this reason, the study of EVOH/diluent phase diagrams is a research subject in polymer science.[4]

The thermally induced phase separation (TIPS) process is one of the most popular methods to study phase separation of the polymer solutions and to develop microporous membranes.[5–7] TIPS can proceed via either solid-liquid (S-L) or liquid-liquid (L-L) phase separation.[8] Solid–liquid phase separation results from the crystallization of the polymer from the homogeneous solution and the driving force for this phase separation is the difference in the chemical potential of the polymer in the crystalline and solution phases.[9] Liquid–liquid phase separation results from the thermodynamic instability of the polymer-solvent system by the decrease of the temperature (upper critical solution temperature – UCST behavior) or from an increase of the temperature (lower critical solution temperature – LCST behavior). For semicrystalline polymers, L-L phase separation is accompanied by simultaneous or subsequent polymer crystallization.[8,10]

Thermodynamics is a powerful tool to describe the phase behavior of solutions allowing prediction of the temperature, composition and shape of phase boundaries, such as the equilibrium melting temperature and crystallization temperature for a semicrystaline polymer in S-L phase separation, as well the spinodal and binodal curves for L-L phase separation.[8]

EVOH copolymers possess a limited miscibility with others polymers, because of the high density of hydrogen interactions between the hydroxyl groups. However, there are not many studies in the literature that attempt to investigate the EVOH tendency to immiscibility in relation to the other polymers

Correspondence to: M. I. Felisberti (misabel@iqm.unicamp.br).

Contract grant sponsor: CNPq, Fapesp.

TABLE I
Properties of EVOH

Polymers	Ethylene (mol %)	Nomenclature	Source	$\overline{M}_w$ (g/mol)[a]	$\overline{M}_n$ (g/mol)[a]	$\overline{M}_w/\overline{M}_n$[a]
EVOH	32	EVOH-32	Aldrich	94,000	65,000	1.5
	38	EVOH-38	Aldrich	95,000	65,000	1.5

[a] GPC in *N*,*N*-dimethylformamide at 313 K.

and solvents. Our research group has been trying to elucidate the possible interactions between EVOH copolymers, with ethylene content in the range of 27–44 mol %, and others polymers, like EVOH/PMMA blends.[11] For this pair, the results from differential scanning calorimetry (DSC) and dynamical mechanical analyses (DMA) show that all the blends prepared by mechanical mixing are heterogeneous.[11] Blends obtained by casting showed a bilayer and porous structure.[12] This behavior could be attributed to unfavorable hydrophobic–hydrophilic interactions involving the ethylene segments of EVOH and the PMMA chains.

The aim of this work is to investigate the phase behavior of EVOH/DMF solutions and to use the binary interaction model[13] to show the importance of considering the internal segment–segment interaction of copolymers in the phase separation behavior of EVOH/DMF solutions. Moreover, the melting point depression method described by Hoffman-Weeks[14] was used to determine the equilibrium melting temperature of the pure EVOH copolymers and EVOH in EVOH/DMF solutions, allowing analysis of the influence of the EVOH composition on the temperature of solid–liquid (S-L) phase separation.

EXPERIMENTAL

The polymers used in this work were commercial products whose properties are listed in Table I.

Preparation of the binary solutions

Defined amounts of EVOH and DMF were added to a tube, heated at 453 K, under constant stirring, and maintained for 2 h to get a homogeneous mixture. The EVOH volumetric fractions (ϕ_{EVOH}) in the binary solutions were 0.08, 0.16, 0.25, 0.34, and 0.44.

Differential scanning calorimeter (DSC)

MDSC 2910 TA Instruments equipment was used to determine the solution dynamic crystallization temperature (Tc_d). The samples was sealed in hermetic aluminum pans and the experiments were performed according to the following program: (a) initial temperature of 303 K; (b) first heating: heating rate of 10 K min^{-1} to 453 K; (c) cooling: cooling rate of 10 K min^{-1} to 248 K; (d) second heating: heating rate of 10 K min^{-1} to 453 K. The results reported in this work correspond to the cooling and second heating runs. All DSC curves were normalized with respect to the sample mass.

Optical microscopy (OM)

The binary solutions were placed between a pair of microscope coverslips. A Teflon ring of 100 μm thickness was used between the coverslips to prevent the evaporation of DMF. The sample was heated on a hot stage at 453 K for 1 min to assure homogeneity. Then it was cooled to 293 K at a controlled rate of 10 K/min. A Linkam CSS-450 controller connected to the Nikon E800 microscope was used to control the temperature. Cloud point temperatures (T_{cloud}) were visually determined by the appearance of turbidity. These experiments were done in triplicate. The loss of solvent during the experiments was gravimetrically monitored and the value was kept around 2%.

Equilibrium melting temperature determination (t_m^0)

Isothermal crystallization was performed on the MDSC 2910 TA Instruments equipment based on the melting point depression method described by Hoffman-Weeks.[14] The experiments were performed for each composition at four different crystallization temperatures (T_c) according to the following program: (a) heating rate of 10 K min^{-1} in the temperature range of 303–453 K; (b) cooling rate of 20 K min^{-1} to desire T_c for each composition, following by an isothermal period of 30 min; (c) heating rate of 10 K min^{-1} to obtain the melting temperature.

RESULTS AND DISCUSSION

Phase diagram determination

Experimental phase diagrams of EVOH-38/DMF and EVOH-32/DMF solutions are shown in Figure 1, through the liquid–liquid (L-L) and solid–liquid (S-L) phase separation temperatures that were

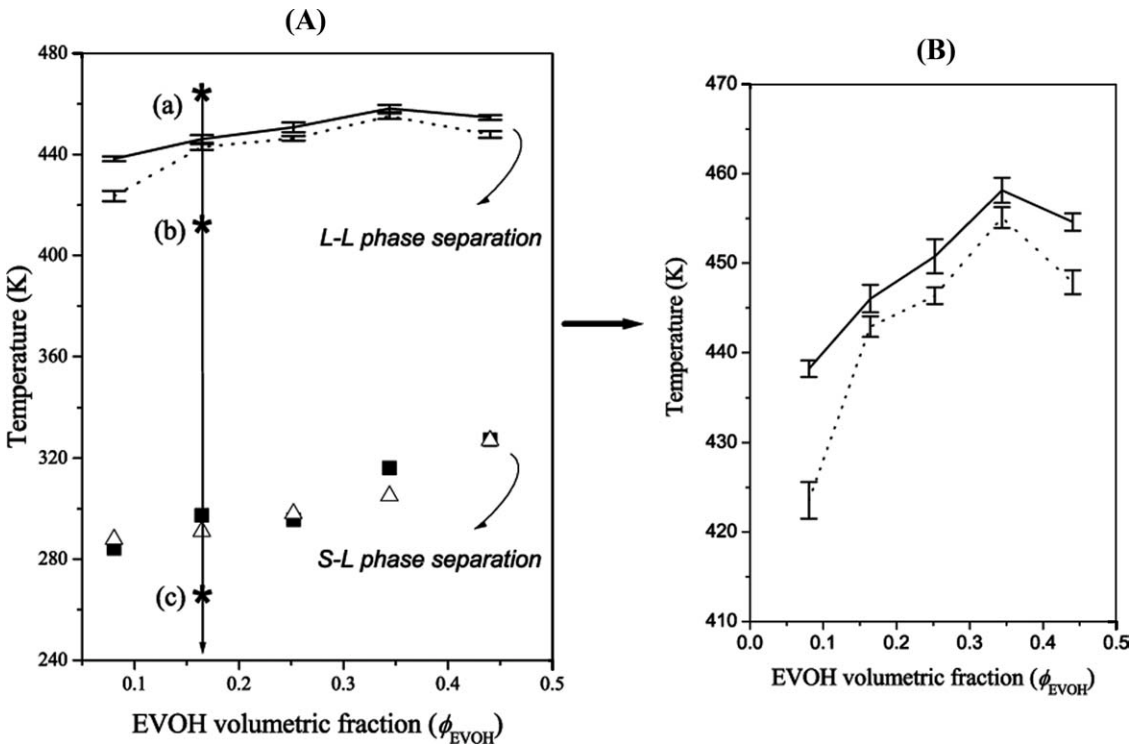

Figure 1 A: Experimental phase diagrams of EVOH/DMF solutions. Cloud points temperatures (T_{cloud}) (——) and (- - -) and dynamic crystallization temperature (Tc_d) (■) and (△) as a function of EVOH volume fraction ((EVOH), for EVOH-38/DMF and EVOH-32/DMF solutions, respectively; B: liquid–liquid phase separation region of EVOH/DMF solutions.

determined by optical microscopy (T_{cloud}) and DSC (Tc_d), respectively.

All the EVOH/DMF solutions are homogeneous at temperatures higher than the cloud points temperatures, point (a) in Figure 1. As the temperature drops, the solution goes from one homogeneous and transparent phase to the situation of phase segregation, a typical UCST- behavior. Moreover, the phase diagram shows that the L-L phase separation takes place before crystallization of EVOH. Thus, point (b) in Figure 1, has coexisting liquid phases and while at point (c) at least one of the phases presents a crystal portion.

At temperatures between the L-L and S-L phase separation lines the EVOH/DMF solutions become a white and very viscous gel. The phases could not be separated, even under centrifugation. Therefore, the composition of the phases could not be determined.

Matsuyama et al.[5] investigated the phase diagrams of the binary solutions, EVOH-32/1,3-propanediol and EVOH-32/1,3-butanediol, with similar concentrations of the EVOH/DMF solutions used in this work. The dynamical crystallization temperature (Tc_d) was determined by DSC measurements. No structure was detected by optical microscopy at temperatures higher than the crystallization temperature. Therefore, the apparent binodal line probably exists in the lower temperature region. According to the authors the porous structures in these two systems were formed by EVOH crystallization rather than by L-L phase separation. EVOH-32/1,3-butanediol solutions showed a dynamic crystallization temperature higher than that of the EVOH-32/1,3-propanediol solutions and this was explained based on the higher difference in solubility parameters (δ) in the EVOH-32/1,3-butanediol solutions in comparison with the value for EVOH-32/1,3-propanediol solutions. This means that the miscibility between EVOH-32 and butanediol is lower, which leads to the higher crystallization temperature. In this case, both the solvents are diols and their hydroxyls can be associated through hydrogen bonding or with the hydroxyl groups of the EVOH chains. This fact does not exclude the possibility of hydrogen bonding between the EVOH chains themselves, which means that there must be a strong competition among the possible combinations of hydroxyls. In the EVOH/DMF solutions a fraction of hydrogen bonding involving hydroxyls is replaced by interactions between the hydroxyls of EVOH and the carbonyls of DMF.

The phase diagram for EVOH/DMF solutions (Fig. 1) shows, for the same composition, that the L-L phase separation curve for EVOH-38/DMF solutions occurs at a slightly higher temperature than for EVOH-32/DMF solutions. As the copolymers have similar molar masses, the difference of the cloud point temperature could be attributed to the solubility parameters of EVOH-38, EVOH-32, and DMF, Table II.

TABLE II
Solubility Parameters[10,15]

Polymer	Solubility parameters [(MPa)$^{1/2}$]
EVOH-32	22.6
EVOH-38	22.0
polyethylene	15.8
poly(vinyl alcohol)	25.8
DMF	24.8

As the ethylene content in EVOH increases the solubility parameter decreases and shows values more distant from DMF, leading to worse affinity.[16] Thus, the line of the L-L phase separation for EVOH-38/DMF solutions may be shifted to higher temperatures compared with EVOH-32/DMF solutions.

In general EVOH-38/DMF and EVOH-32/DMF solutions crystallize at similar temperatures. However, EVOH-32 has a concentration of hydroxyl groups higher than EVOH-38, increasing the density of hydrogen interactions for the pair EVOH-32 and DMF. At the same time, the increase in the amount of hydroxyl groups encourages EVOH self crystallization from solution.

The phase behavior of EVOH/DMF solutions seems to be more complex in comparison with EVOH/diols solutions, reported by Matsuyama et al.[5] EVOH/DMF solutions present L-L phase separation followed by crystallization of EVOH, probably in a liquid phase richer in EVOH. While the EVOH/diols solutions undergo S-L phase separation in the temperature range around 373 K, higher than that observed for EVOH/DMF solutions.

To better understand the role of interactions between ethylene and the hydroxyls in vinyl alcohol and between ethylene and DMF on the phase behavior of EVOH/DMF solutions, the binary interaction model, proposed by Paul and Barlow[13] to predict the miscibility of blends formed by homopolymers and copolymers was used. Similarly, this model was successfully used by Lv et al.[17] to predict the phase behavior of EVOH/1,4-butanediol, EVOH/1,3-propanediol and EVOH/glycerol solutions, considering the intermolecular and intramolecular interactions.

Binary interaction model

As far as the phase behavior of copolymer mixtures is concerned, both intermolecular and intramolecular interactions of component units of copolymers should be considered. The existence of the window of miscibility in copolymer-homopolymer blends has been rationalized in thermodynamic terms by means of a binary interaction model and other similar approaches.[13] In the case of copolymer-diluent systems like EVOH/DMF, the binary interaction model could be used, replacing the homopolymer by the solvent, DMF. This model considers the intermolecular and intramolecular interactions between the ethylene (Et) and vinyl alcohol (VA) segments imposed by the covalent bond in EVOH.[17]

The binary interaction model for the heat of mixing can be extended to a multicomponent mixture as follows[9]:

$$\frac{\Delta H_m}{V} = \sum_{i>j} B_{ij}\phi_i\phi_j \tag{1}$$

where V is the total molar volume of the mixture $= \left(\sum_{i>j} V_i\right)$. The right side of eq. (1) excludes terms with $i = j$ and double counting of terms with i different from j. B is the binary interaction energy density[12] and is also related to the Flory-Huggins interaction parameter, χ, by:

$$B = RT\frac{\chi}{V_1} \tag{2}$$

where V_1 is the molar volume of the solvent.

According to the concept of binary interactions, for a binary mixture of random copolymer EVOH, consisting of comonomer 1 (ethylene) and

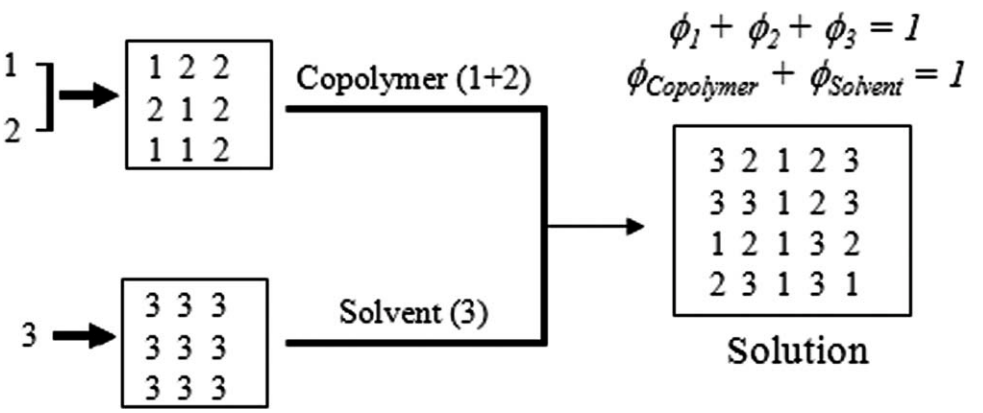

Figure 2 Scheme of the binary interaction model for the physical situation involving a copolymer in solution.[12]

TABLE III
Hansen Solubility Parameter for Ethylene, Vinyl Alcohol, and DMF[18]

Material	δ_d (MPa)$^{1/2}$	δ_p (MPa)$^{1/2}$	δ_h (MPa)$^{1/2}$
Vinyl alcohol	16.0	14.3	23.9
Ethylene	17.0	0	0
Dimethyformamide	17.2	15.6	21.3

comonomer 2 (vinyl alcohol), and a solvent 3 (DMF), the scheme of the physical situation of the solutions may be represented by Figure 2.

Thus, the binary interaction energy density B can be expressed by:

$$B = \sum_{i>j}^{\text{Inter}} B_{ij}\phi_i\phi_j - \sum_{i>j}^{\text{Intra}} B_{ij}\phi_i\phi_j = B_{13}\phi_1 + B_{23}\phi_2 - B_{12}\phi_1\phi_2 \quad (3)$$

where B_{12}, B_{13} and B_{23} are the interaction energy densities between 1 and 2, 1 and 3 and 2 and 3, respectively. For the estimation of these B, Hansen solubility parameters[18] are applied to get more accurate values.

$$B_{ij} = (\delta_{di} - \delta_{dj})^2 + 0,25(\delta_{pi} - \delta_{pj})^2 + 0,25(\delta_{hi} - \delta_{hj})^2 \quad (4)$$

The solubility parameter components δ_d, δ_p and δ_h represent the strength dispersion, dipolo moment and the contributions of polar groups, respectively.[18] Equation (4) predicts only positive values for B and consequently for χ [eq. (2)]. Table III lists the solubility parameters of the comonomers and solvent.

The values of inter- and intrasegmental binary interaction energy densities, B_{ij}, were obtained according to eq. (4). The evolution of the B term with the vinyl alcohol (VA) volume fraction in the copolymer can be calculated using eq. (3). All these values are listed in Table IV.

Intersegmental B ($B_{\text{Et/DMF}}$ and $B_{\text{VA/DMF}}$) and intrasegmental B ($B_{\text{Et/VA}}$) are considered independent of the composition of the solution. Figure 3 shows the B values as a function of EVOH volume fraction in the EVOH/DMF solutions.

EVOH-38/DMF solutions show B, and therefore χ, values higher than EVOH-32/DMF solutions. This difference between the values for both solutions with comparable concentrations increases as the amount of EVOH increases. The binary interaction model provides that the L-L phase separation for EVOH-38/DMF solutions is located at higher temperatures and not occur only as a consequence of hydrogen bonding between the hydroxyls of EVOH, but also by interactions between Et and VA and interactions between the comonomers (Et and VA) and DMF (Table IV).

The interactions between VA and DMF should be responsible for the solubility of EVOH in DMF at high temperatures, as B_{23} shows a lower value than B_{12} and B_{13}. As can be seen, the binary interaction model appropriately describes the experimental data (Fig. 1) in the sense that copolymers with lower VA content (EVOH-38) should be more immiscible with DMF.

Equilibrium melting temperature determination

The experimental data shows an increase in the dynamic crystallization temperature of EVOH with the increase of copolymer in the binary solutions, Figure 1. In the same way, the melting temperature (T_m) decreases as the EVOH concentration decreases in the EVOH/DMF solutions, Figure 4, as consequence of the chemical potential.

The depression of the melting point may be explained in terms of thermodynamic mixing, by the exothermic interaction between a crystalline polymer-solvent and by two other effects: (i) the kinetic effects associated with the presence of crystals formed at temperatures below the crystallization isothermal temperature; and (ii) the morphologies that are associated with changes in crystal perfection or geometry and with different thermal histories of the sample.[12,19,20]

Apparently, there is no difference between the T_m of EVOH/DMF solutions for both copolymers.

TABLE IV
Intersegmental and Intrasegmental Binary Interaction Energy Densities for EVOH/DMF Solutions

Copolymer	Solvent	$B_{\text{Et/VA}}$ (J m^{-3})	$B_{\text{Et/DMF}}$ (J m^{-3})	$B_{\text{VA/DMF}}$ (J m^{-3})	ϕ_{Et}	ϕ_{VA}	ϕ_{DMF}	B (J m^{-3})
EVOH-38	DMF	196.48	174.42	3.55	0.03	0.05	0.92	5.12
(Et38/AV/DMF)		196.48	174.42	3.55	0.06	0.10	0.84	9.64
		196.48	174.42	3.55	0.09	0.16	0.75	13.44
		196.48	174.42	3.55	0.13	0.21	0.66	18.06
		196.48	174.42	3.55	0.17	0.27	0.56	21.60
EVOH-32	DMF	196.48	174.42	3.55	0.03	0.05	0.92	5.12
(Et32/AV/DMF)		196.48	174.42	3.55	0.05	0.11	0.84	8.03
		196.48	174.42	3.55	0.08	0.17	0.75	11.88
		196.48	174.42	3.55	0.11	0.23	0.66	15.03
		196.48	174.42	3.55	0.14	0.30	0.56	17.23

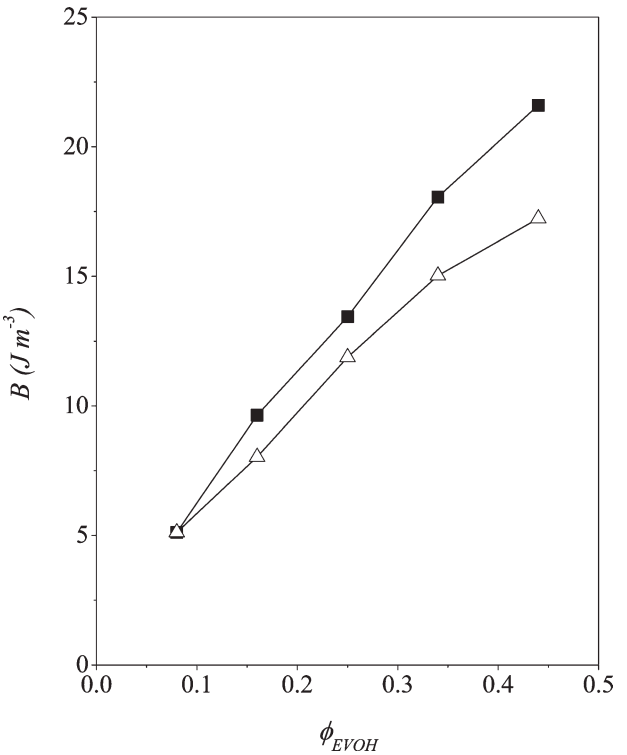

Figure 3 Binary interaction energy density (B) as a function of EVOH volume fraction (φ_{EVOH}) for the binary solutions: (■): EVOH-38/DMF and (△) EVOH-32/DMF.

However, the values should also reflect the kinetic and morphological effects. To analyze the influence of the ethylene content on the melting temperature these effects were removed or minimized by construction of the Hoffman–Weeks plot, using the melting temperature as a function of crystallization temperature for pure EVOH and for EVOH in the solutions isothermally crystallized at different temperatures (T_c).[18]

According to the phase diagram, Figure 1, the solid-liquid phase separation occurs at the L-L phase separation region. In principle, EVOH could crystallize in both phases, but the phase richer in EVOH crystallizes at higher temperature. Thus, the observed crystallization was due to the EVOH crystallization in the phase richer in EVOH. Moreover, there is no evidence of further crystallization at temperatures below 284 K, which means that the crystallization of the lean phase in EVOH was not detected.

The isothermal crystallization was performed in four different temperatures. However, the temperatures do not differ from each other more than 3 K. Thus, the composition of the more viscous phase (phase richer in EVOH) should not differ significantly. This hypothesis is reinforced by the observation of good data correlations shown in Figure 5.

The equilibrium melting temperature, T^0_{me} and T_{me}, for pure EVOH and EVOH in the solutions, respectively, are determined by the extrapolation of the experimental curve to the curve corresponding to $T_m = T_c$, Figure 5, assuming perfect crystals with finite size and fully chain extended. Moreover, there is no recrystallization during the melting run.[19,21]

The equilibrium melting temperatures (T^0_{me}) obtained for pure EVOH-38 and EVOH-32 are 455 K and 460 K, respectively. The equilibrium melting temperatures (T_{me}) for the EVOH/DMF solutions as a function of the EVOH volume fraction is shown in Figure 6.

Figure 6 shows that the equilibrium melting temperature of the solutions increases with the increase of EVOH volume fraction in the solution. This effect is more pronounced for EVOH-32/DMF solutions, which means that there is an influence of the vinyl alcohol content in EVOH during the melting. In general, higher melting temperature of a polymer can be due to higher lamellar thicknesses.[22] Thus, the higher melting temperature of the EVOH-32 in comparison with EVOH-38 in the solutions is due to the higher amount of vinyl alcohol segments and, consequently, to the higher lamellar thicknesses of the vinyl alcohols crystals.

Morphology of the EVOH/DMF solutions

EVOH-32/DMF and EVOH-38/DMF solutions containing $\phi_{EVOH} = 0.16$ and $\phi_{DMF} = 0.84$ were

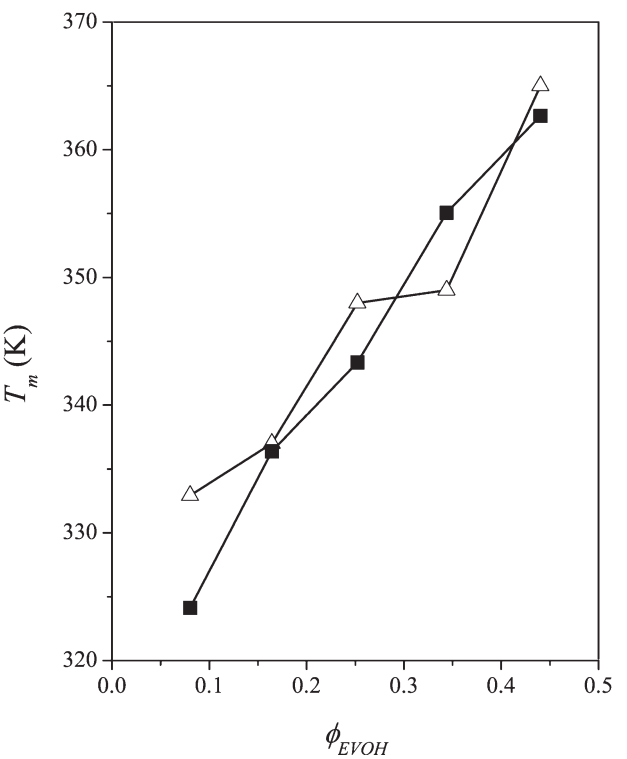

Figure 4 Melting temperature (T_m) obtained, at a heating rate of 10 K min^{-1}, as a function of EVOH volume fraction (φ_{EVOH}): (■) EVOH-38/DMF and (△) EVOH-32/DMF.

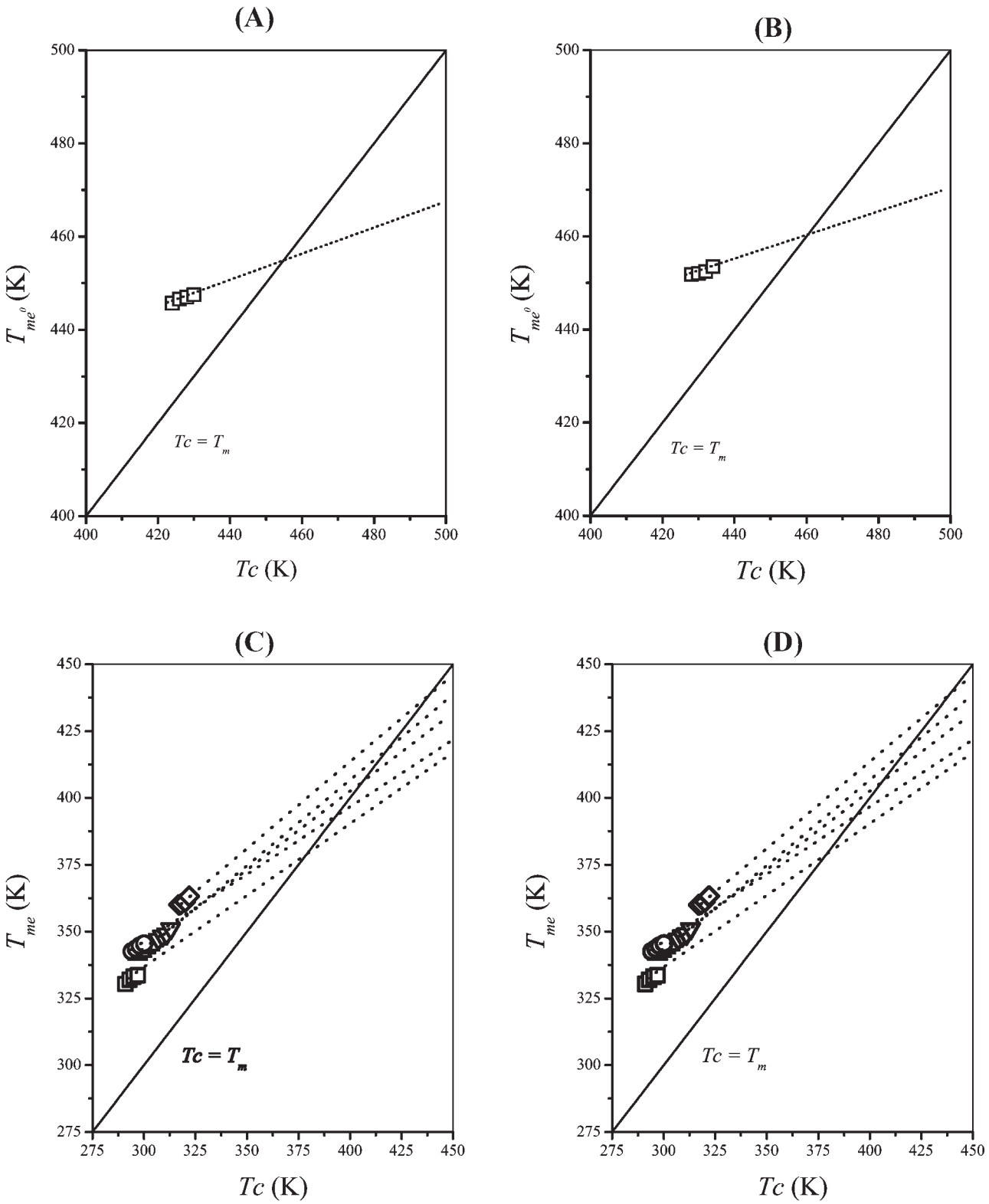

Figure 5 Hoffman-Weeks plots for EVOH isothermally crystallized in the solutions: (A) EVOH-38 and (B) EVOH-32, (C) EVOH-38/DMF, and (D) EVOH-32/DMF. EVOH volume fraction (ϕ_{EVOH}): (□) 0.08; (○) 0.16; (△) 0.25; (▽) 0.34 and (□) 0.44.

submitted to the same cooling program from 453 K to investigate the L-L phase separation by the TIPS process through optical microscopy. The samples were cooled from the homogeneous region at cooling rate of 10 K min^{-1} to a desired temperature and kept for 20 min in the indicated temperature. Figure

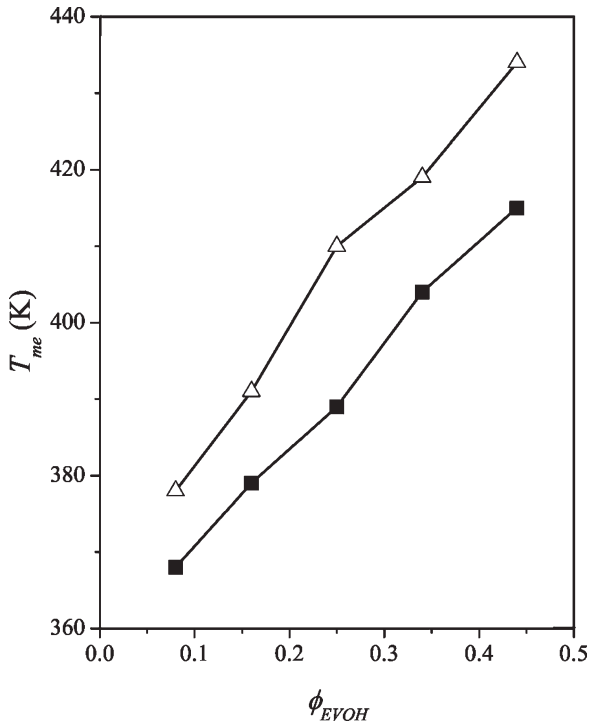

Figure 6 Equilibrium melting temperature (T_{me}) obtained by Hoffman-Weeks plots for EVOH isothermally crystallized in the solutions, as a function of EVOH volume fraction (φ_{EVOH}): (■) EVOH-38/DMF and (△) EVOH-32/DMF.

7 shows the micrographs of EVOH/DMF solutions at different temperatures in the phase diagram region between the L-L and S-L lines.

The morphology of EVOH-32/DMF and EVOH-38/DMF solutions at 378 K indicates interconnected and continuous phases, which are typical of phase separation by the spinodal decomposition mechanism and is related to the L-L phase separation by the TIPS process. The micrographs at 343 K show an increase in the contrast between the interconnected phases formed due to the higher difference in the phases compositions. However, the dimensions of the phases seem not to change probably due to the formation of a gel phase, rich in EVOH. Thus, there is no coalescence of the phases during the experiments. All EVOH/DMF solutions with different compositions showed similar behavior.

CONCLUSIONS

Binary solutions, EVOH/DMF, showed phase separation with a decrease of the temperature, UCST behavior. The L-L phase separation was observed at temperatures higher than EVOH crystallization, possibly as a result of the competition between hydrogen bonding of the hydroxyls in EVOH chains and

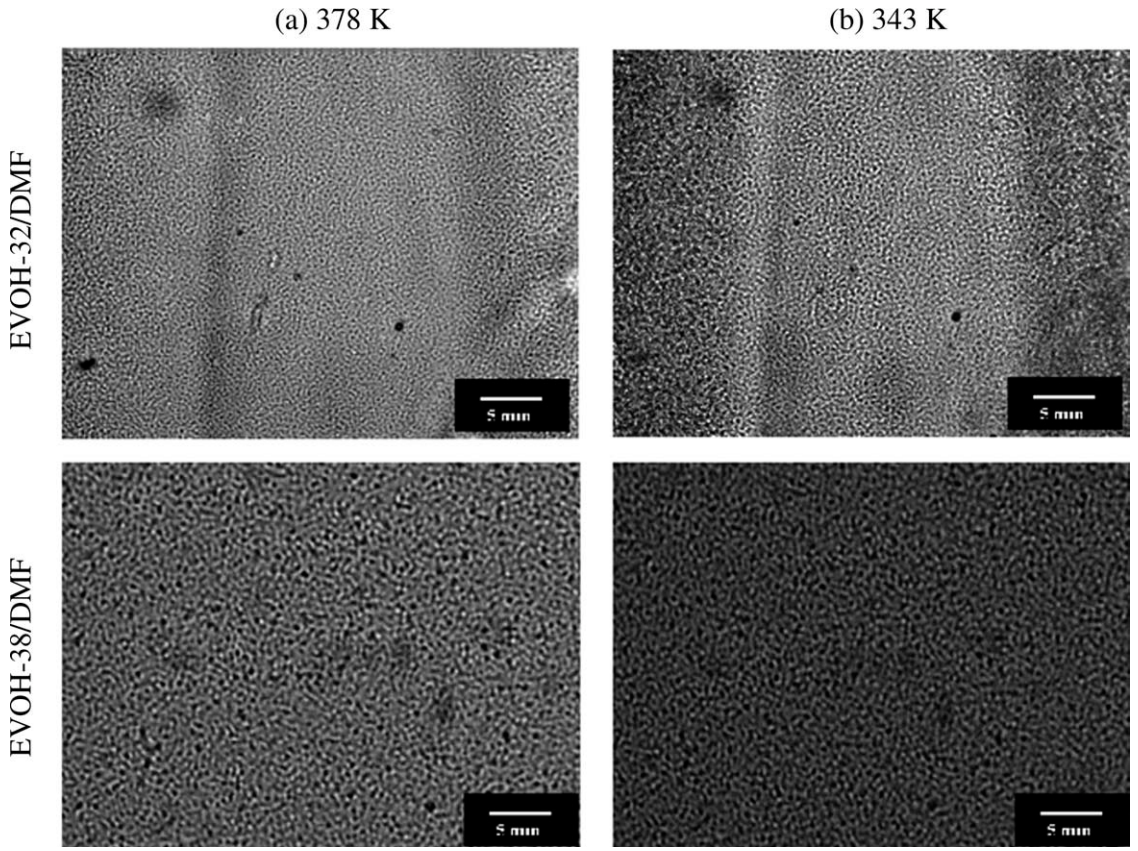

Figure 7 Optical micrographs of EVOH/DMF solutions, containing $\varphi_{EVOH} = 0.16$ and $\varphi_{DMF} = 0.84$, as a function of temperature. Cooling rate of 10 K/min.

between the hydroxyls and carbonyls in EVOH and DMF, respectively. Moreover, as the ethylene content in EVOH increases the solution becomes less miscible, because of the lower affinity between the copolymer and solvent. The binary interaction model provides L-L phase separation for EVOH-38/DMF solutions at temperatures higher than for EVOH-32/DMF solutions, which describes appropriately the experimental phase diagram obtained. This result indicates that the copolymers with lower VA content should be more immiscible with DMF. The equilibrium melting temperature of pure EVOH-32 is higher than pure EVOH-38. The same behavior is observed in their binary solutions, which reflects the influence of the vinyl alcohol content in EVOH during melting.

The authors are grateful to Dr. C.H. Collins for manuscript revision.

References

1. Villar, M. A.; Thomas, E. L.; Armstrong, R. C. Polymer 1995, 36, 1869.
2. Matsuyama, H.; Kobayashi, K.; Maki, T.; Tearamoto, M. J Appl Polym Sci 2001, 82, 2583.
3. Lagarón, J. M.; Gimenez, E.; Saura, J. J.; Gavara, R. Polymer 2001, 42, 7381.
4. Horst, R. Macromol Theory Simul 1996, 5, 789.
5. Matsuyama, H.; Iwatani, T.; Kitamura, Y.; Tearamoto, M.; Sugoh, N. J Appl Polym Sci 2001, 79, 2449.
6. Tsai, F.-J.; Torkelson, J. M. Macromolecules 1990, 23, 775.
7. Lv, R.; Zhou, J.; Du, Q.; Wang, H.; Zhong, W. J Membr Sci 2006, 281, 700.
8. Olabisi, O.; Robeson, L. M.; Shaw, M. T. Polymer–Polymer Miscibility; Academic Press: New York, 1979.
9. Flory, P. J. Principles of Polymer Chemistry; Cornell University Press: Ithaca, New York, 1953.
10. Shang, M.; Matsuyama, H.; Maki, T.; Teramoto, M.; Lioyd, D. R. J Appl Polym Sci 2003, 87, 853.
11. Lima, J. A.; Felisberti, M. I. Eur Polym J 2008, 44, 1140.
12. Lima, J. A.; Felisberti, M. I. J Membr Sci 2009, 344, 237.
13. Paul, D. R.; Barlow, J. W. Polymer 1984, 25, 487.
14. Hoffman, J. D.; Weeks, J. J. J Res Natl Bur Stand 1962, 66, 13.
15. Brandrop, J.; Immergut, E. H. In Polymer Parameters Handbook; Wiley: New York, 1989.
16. Matsuyama, H.; Tearamoto, M.; Kudari, S.; Kitamura, Y. J Appl Polym Sci 2001, 82, 169.
17. Lv, R.; Zhou, J.; Xu, P.; Du, Q.; Wang, H.; Zhong, W. J Appl Polym Sci 2007, 105, 3513.
18. Hansen, C. M. Hansen Solubility Parameters; CRC Press: Boca Raton, 2000.
19. Huo, P. P.; Cebe, P. Macromolecules 1993, 26, 3127.
20. Nishi, T.; Wang, T. T. Macromolecules 1975, 8, 909.
21. Cimmino, S.; Martuscelli, E.; Silvestre, C.; Canetti, M.; De Lalla, C.; Seves, A. J Polym Sci: Polym Phys 1989, 27, 1781.
22. Gedde, W. U. Polymer Physics; Chapman and Hall: New York, 1995; p 138.